Role of high-resolution ultrasound and magnetic resonance neurography in the evaluation of peripheral nerves in the upper extremity

Ali Serhal[1] , Steven Kyungho Lee[1] , Julia Michalek[2] , Muhamad Serhal[1] ,
Imran Muhammad Omar[1]

[1] Department of Radiology, Northwestern University, Chicago, USA
[2] Department of Radiology, Northwestern Memorial Hospital, Chicago, USA

Corresponding author: Ali Serhal; e-mail: ali.serhal@northwestern.edu

Abstract

Upper extremity entrapment neuropathies are common conditions in which peripheral nerves are prone to injury at specific anatomical locations, particularly superficial regions or within fibro-osseous tunnels, resulting in pain and potential disability. Although neuropathy is primarily diagnosed clinically by physical examination and electrophysiology, imaging evaluation with ultrasound and magnetic resonance neurography are valuable complementary non-invasive and accurate tools for evaluation and can help define the site and cause of nerve dysfunction which ultimately leads to precise and timely treatment. Ultrasound, which has higher spatial resolution, can quickly and comfortably characterize the peripheral nerves in real time and can evaluate for denervation related muscle atrophy. Magnetic resonance imaging on the other hand provides excellent contrast resolution between the nerves and adjacent tissues, also between pathologic and normal segments of peripheral nerves. It can also assess the degree of muscle denervation and atrophy. As a prerequisite for nerve imaging, radiologists and sonographers should have a thorough knowledge of anatomy of the peripheral nerves and their superficial and deep branches, including variant anatomy, and the motor and sensory territories innervated by each nerve. The purpose of this illustrative article is to review the common neuropathy and nerve entrapment syndromes in the upper extremities focusing on ultrasound and magnetic resonance neurography imaging.

Introduction

Peripheral neuropathies are common, with a reported prevalence ranging from 2.4% in the general population to 8% in elderly patients[1]. They cause a variety of sensory, motor, autonomic or mixed symptoms, and are classified as noncompressive and compressive (entrapment) neuropathies[2]. The most common causes of noncompressive neuropathy worldwide are diabetes mellitus, hypothyroidism, and nutritional deficiencies[3], in addition to leprosy, which is still prevalent in India, Africa, and Southeast Asia. In contrast, compressive neuropathies are caused by traction, entrapment or an intrinsic nerve lesion, especially in the upper limbs at specific vulnerable locations, where the nerve may be superficially located or course through fibromuscular or bony tunnels. Carpal tunnel syndrome is the most common entrapment neuropathy with an annual incidence of 1 in 1,000 in the general population[4]. Although peripheral neuropathies are primarily clinical diagnoses that rely on physical examination and electrodiag-

nostic testing, such as nerve conduction velocities and electromyography, imaging can play an important role in confirming the diagnosis, determining the location of nerve abnormalities, detecting abnormalities that can result in compressive neuropathy, assessing the degree of associated findings such as muscle pathology, and to detect conditions that can result in overlapping symptoms, such as tendinopathy. The purpose of this article is to show the role of imaging in the evaluation of the peripheral nerves in the upper extremities.

Imaging modalities and normal nerve anatomy

Ultrasonography (US) and magnetic resonance neurography (MRN) are the most common imaging modalities used to assess peripheral nerves and are complementary to clinical assessment and electrodiagnostic testing in diagnosing and managing peripheral neuropathies (Fig. 1).
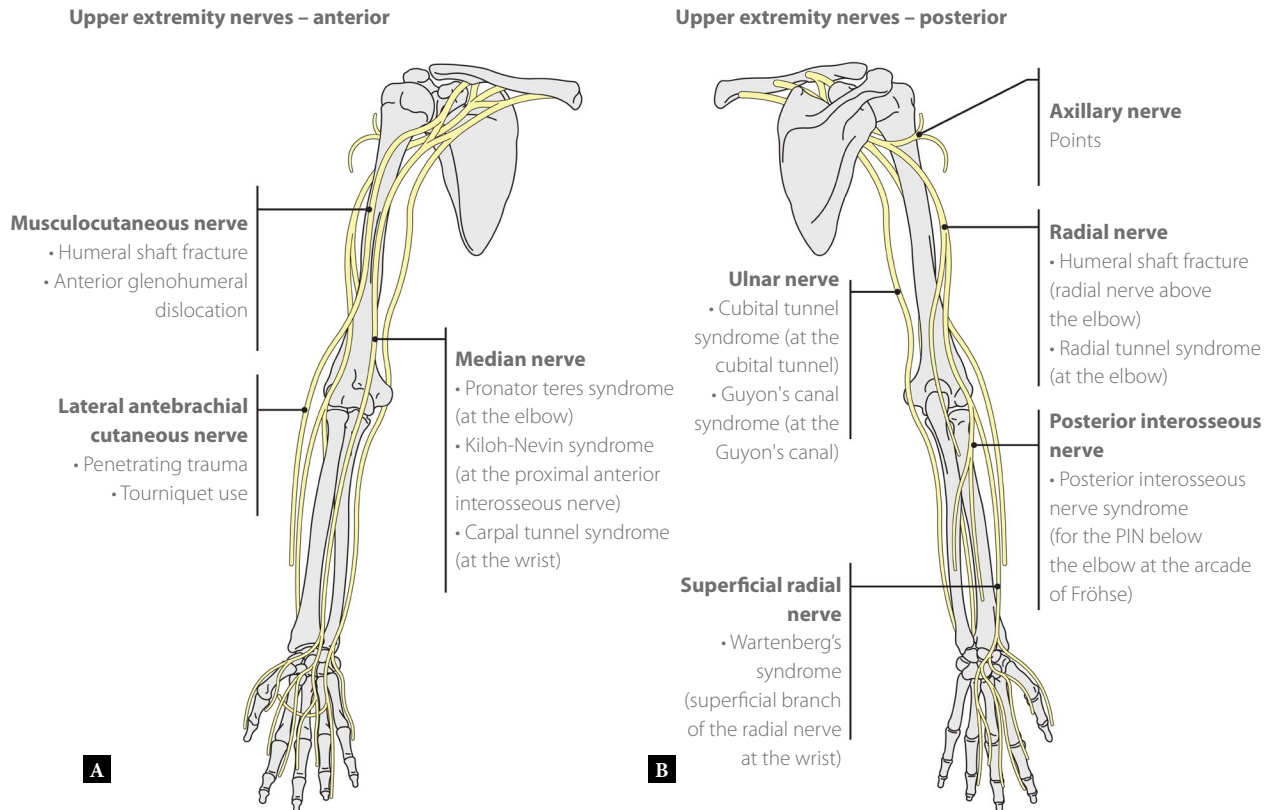
Upper extremity nerves – anterior

Upper extremity nerves – posterior

Musculocutaneous nerve
• Humeral shaft fracture
• Anterior glenohumeral dislocation

Lateral antebrachial cutaneous nerve
• Penetrating trauma
• Tourniquet use

Median nerve
• Pronator teres syndrome (at the elbow)
• Kiloh-Nevin syndrome (at the proximal anterior interosseous nerve)
• Carpal tunnel syndrome (at the wrist)

Axillary nerve
Points

Radial nerve
• Humeral shaft fracture (radial nerve above the elbow)
• Radial tunnel syndrome (at the elbow)

Ulnar nerve
• Cubital tunnel syndrome (at the cubital tunnel)
• Guyon's canal syndrome (at the Guyon's canal)

Posterior interosseous nerve
• Posterior interosseous nerve syndrome (for the PIN below the elbow at the arcade of Fröhse)

Superficial radial nerve
• Wartenberg's syndrome (superficial branch of the radial nerve at the wrist)

A **B**

Fig. 1. A. *Anterior and* **B.** *Posterior diagrams of major upper extremity peripheral nerves with associated clinical conditions*

Ultrasound

Upper extremity peripheral nerves are best assessed with high-frequency (>15 MHz) linear probes[5]. Nerves are composed of alternating hypoechoic nerve fascicles, which are usually of similar size and echogenicity, and echogenic connective tissue, corresponding to the endoneurium, perineurium and interfascicular epineural fat. This arrangement has a "honeycomb" pattern when scanning a normal nerve in the transverse/short axis (Fig. 2). Long-axis imaging of the nerve shows a longitudinal fascicular pattern. As opposed to nerves, tendons usually present with numerous, thinner, and more densely packed echogenic lines alternating with hypoechoic lines, resulting in a fibrillar pattern that helps differentiate them from nerves[6].

Sonographic findings of abnormal nerves may depend on whether there is noncompressive or compressive neuropathy. In noncompressive neuropathies, there is usually involvement of a longer nerve segment compared to compressive neuropathies, where the nerve appears larger proximal to the site of compression, often with fascicular thickening, and relatively abrupt flattening at the site of compression. Abnormal nerves may demonstrate loss of the normal fascicular pattern with decreased nerve echogenicity secondary to edematous intraneural changes, and may be associated with increased vascularity on Doppler ultrasound, irrespective of the cause[6]. Newer microvascular Doppler techniques detect slower blood flow, which may better identify abnormal intraneural and perineural hyperemia.

Neuropathies of motor nerves often result in muscle denervation changes that are specific to the involved nerve, and the pattern of
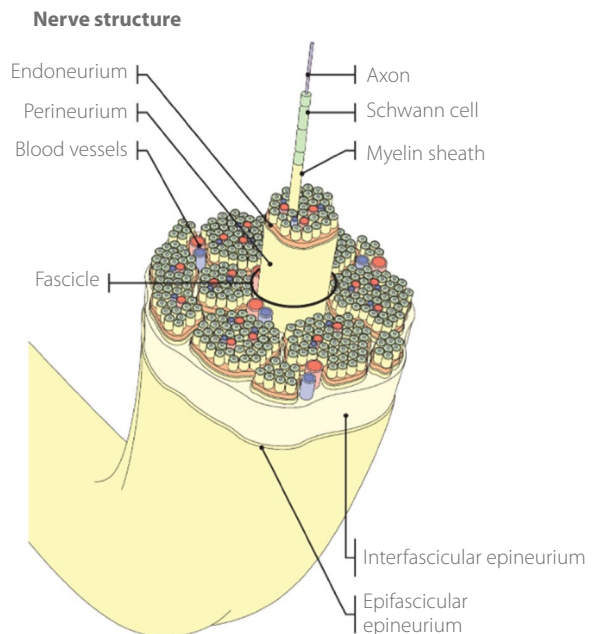
Nerve structure

Endoneurium
Perineurium
Blood vessels
Fascicle
Axon
Schwann cell
Myelin sheath
Interfascicular epineurium
Epifascicular epineurium

Fig. 2. *Diagram illustrating the structural anatomy of a peripheral nerve*

muscle abnormalities is a secondary finding that can suggest abnormality of a particular peripheral nerve. Acute muscle changes may be difficult to detect on US. However, US is excellent at detecting atrophy and fatty replacement of muscles in the innervated territory.

Both US and MRN are complementary examinations for evaluation of peripheral neuropathy. US has some advantages over MRN. These include examining the nerve in real time, the relative shorter scan time, the ability to adapt the field of view of the exam depending on the clinical indication, and the capability to provide dynamic imaging of the nerve with movement and assessing the nerve mobility in cases of entrapment[7]. Furthermore, US provides a quick comparison with the contralateral side, which can serve as an internal control in cases of unilateral symptoms, to better detect subtle nerve and muscle abnormalities. Finally, US can be used to guide perineural anesthetic injection, a well-established technique amongst anesthesiologists to achieve regional anesthesia for upper extremity surgery[8]. Radiologists also often perform upper extremity peripheral nerve perineural injections for diagnostic purposes utilizing local anesthetic or for therapeutic purposes utilizing steroids[9].

Shear-wave elastography (SWE) measures the propagation speed of shear waves generated within tissues to provide quantitative information about tissue stiffness, and can be applied in peripheral nerve imaging[10]. SWE can be utilized to assess the mechanical properties of peripheral nerves and detect areas of nerve compression. Kantarci *et al.* demonstrated that patients with carpal tunnel syndrome have significantly higher median nerve stiffness at the carpal tunnel inlet, and SWE seems to be a reliable diagnostic method with good reproducibility for this condition[11].

Prior to scanning particular peripheral nerves, radiologists and sonographers must know the anatomy in detail, including nerve branching patterns, and be familiar with common anatomic variants. It is advised to start the examination from known anatomic landmarks near the nerve, with the evaluation initially performed in the short axis. Once the nerve is identified, it can be tracked proximally and distally using the so-called "elevator technique" (Video 1). If pathology is encountered (abnormal echogenicity, size or fascicular pattern), then the examination can be focused on that particular segment. Subsequently, the nerve and any associated pathology can be evaluated in the long axis. Ultrasound gel should be used liberally, especially at skin folds. The image quality should be optimized by changing the focal zone and the depth of insonation. Occasionally, particularly for smaller nerves that may be difficult to see reliably in the short axis, rotating the US probe into the long-axis plane after a small segment of the nerve is identified in the short axis may be helpful to characterize the nerve. Finally, caution should be used when applying transducer pressure over the nerve of interest, since this may prevent detecting abnormal nerve movement during stress maneuvers, or reduce blood flow to abnormal nerve segments on Doppler imaging.

Magnetic resonance neurography (MRN)

High field strength systems (3 tesla (T) or higher) with strong magnetic gradients and coils dedicated to the anatomy of interest help to optimize imaging[12]. MRN consists of a combination of "anatomic", high-resolution, nonfat-suppressed (NFS) anatomical sequences, such as T1-weighted (T1W) or proton density-weighted (PDW) sequences, and fat-suppressed (FS), high resolution fluid-sensitive sequences, such as T2-weighted (T2W) or short tau inversion recovery (STIR) sequences in several planes. Most commonly, these are performed with two-dimensional (2D) fast spin echo techniques. An anatomic sequence is commonly performed at least in the short-axis plane and is useful to contrast the difference between the nerve and surrounding fat. This helps to see the morphology and caliber of the nerve and its nerve fascicles, as well as its relationships to surrounding structures. Fat-suppressed, fluid-sensitive sequences accentuate the contrast differences between nerves and background soft tissues to detect signal abnormalities that can indicate nerve pathology, and many centers use heavily T2-weighted, high echo time sequences to increase the contrast between the nerves and background tissues. These sequences are usually performed in multiple planes to better characterize nerve findings in areas of complex anatomy. Since nerves and blood vessels often travel in neurovascular bundles and both structures can be hyperintense to background tissues on fluid-sensitive sequences, it can be difficult to discriminate between them, especially more distally as the nerves become very thin. The NFS anatomic sequence can serve as a roadmap to determine the location of target nerves on more T2 contrasted, FS pulse sequences.

Three-dimensional (3D) spin echo sequences may also be helpful to depict nerves with optimal planes of imaging and can be performed with or without fat-suppression and with various weightings. Some clinically available 3D techniques, including three-dimensional inversion recovery turbo spin echo (3DIRTSE), nerve-SHeath signal increased with INKed rest-tissue RARE Imaging (SHINKEI) and post contrast 3D STIR Sampling Perfection with Application optimized Contrast (SPACE) sequences, have vascular suppression to help better visualize the nerves[13]. The MRN protocol used at our institution is summarized in Tab. 1.

As in US, a normal nerve has a fascicular pattern on MRN, with signal intensities similar to skeletal muscle on T1W images and similar to or slightly brighter than muscle on T2W images. In both compressive and noncompressive neuropathies, there is loss of the normal fascicular pattern of the nerve with increased signal on fluid-sensitive sequences. In cases of entrapment neuropathies, there is enlargement of the compressed nerve proximally with focal flattening at the site of compression. MRN is better than US at showing subacute muscle denervation such as diffuse muscular edema, which is reversible, and detecting irreversible atrophy and fatty infiltration when there is chronic muscle denervation.

Functional MRN with the use of diffusion-weighted imaging (DWI) and diffusion tensor imaging (DTI) can be complementary to morphologic MRN and provide pathophysiologic information about the functional integrity of peripheral nerves or water molecule flow

Tab. 1. MR neurography protocol used for upper extremity evaluation. The field of view is adjusted depending on the indication

Sequence	Echo time	Repetition time	Slice thickness	Flip angle	Acquisition matrix
Axial T1	10	619	3 mm	140	336\0\0\286
Axial T2 FS	104	4000	3 mm	130	256\0\0\230
Coronal STIR	49	4000	3 mm	130	272\0\0\403
Space 3D STIR post contrast	252	3000	isotropic	variable	0\384\252\0

within nerve axons, and to assess surgical procedures[14]. Specific technical adjustments can be performed to obtain high-quality images of peripheral nerves, which, when added to the routine morphologic MRN sequences improve the detection and characterization of peripheral neuropathies. Quantitative parameters, derived especially from DTI neurography, including fractional anisotropy, mean diffusivity, axial diffusivity, and radial diffusivity, allow detection of signal intensity changes in injured or repaired peripheral nerves, and provide pathophysiologic information about the extracellular space, fiber organization, axonal flow, or myelin integrity. Functional MRN has the potential to improve treatment selection, monitor therapeutic response, and predict the healing potential of injured peripheral nerves.

Upper extremity neuropathies

Axillary nerve

The axillary nerve arises from the posterior cord of the brachial plexus. At the level of the shoulder, it splits into anterior and posterior divisions within the quadrilateral space after descending inferolaterally. The posterior division is usually located more superficially and is firmly related to the inferior glenoid rim[15]. The quadrilateral space is bounded superiorly by the teres minor muscle, inferiorly by the teres major muscle, medially by the long head of the triceps muscle, and laterally by the medial aspect of the humerus.

Axillary nerve compression most commonly occurs as it passes through the quadrilateral space, which is known as quadrilateral space syndrome (QSS), and the most frequent cause of QSS is a fibrous band between the long head of the triceps muscle and the teres major muscle or the humerus. Other causes include space-occupying lesions within the quadrilateral space, such as paralabral cysts arising from the inferior glenoid labrum, varicose veins, lymphadenopathy, ganglion cysts, benign tumors, such as lipomas, axillary schwannomas, and humeral osteochondromas, and muscle hypertrophy, especially of the triceps muscle in competitive overhead athletes[15]. In addition to QSS, the axillary nerve can sustain traumatic injuries resulting from anterior glenohumeral dislocation, proximal humeral fracture, direct anterolateral blow to the deltoid muscle or compression by maintaining an extended abducted and externally rotated position of the arm during surgery or by the prolonged uses of the crutches[16]. Usually, patients experience paresthesias and pain in the posterolateral area of the shoulder, exacerbated by abduction and external rotation, with loss of motor function and muscle atrophy in more advanced cases[17].

Due to the nerve's small size and deeper location, US usually has a limited role in diagnosing axillary neuropathy. The axillary nerve supplies the deltoid, teres minor and triceps lateral head muscles, and fatty atrophy of these muscles should suggest neuropathy of this nerve. Although it can be difficult to see on US, this nerve courses adjacent to the posterior circumflex humeral artery, which can be used as a sonographic landmark and can be identified by color Doppler imaging[18]. Dynamic US can be helpful to detect cases of compression that occur exclusively during abduction and external rotation, and loss of flow in the axillary artery on Doppler imaging can also serve as an additional, indirect sign of axillary nerve compression. Comparison with the contralateral side may help confirm the

diagnosis in less obvious cases[19]. MRN or computed tomography angiography (CTA) can show similar vascular findings and requires image acquisition in the neutral position and during arm movement. Additionally, US-guided axillary nerve block is frequently used as a pain-relieving technique.

MRN can help to detect the direct signs of axillary neuropathy, including nerve edema or changes in caliber, as well as any space-occupying lesions. While space-occupying lesions in the quadrilateral space are readily visible on MRN, fibrous bands can be difficult to see directly and may be inferred if there is an abrupt caliber change in the nerve. MRN is superior to US at detecting the pattern of deltoid and teres minor muscle denervation edema reflecting axillary neuropathy, though isolated posterior branch neuropathy may only result in teres minor involvement (Fig. 3). Sofka *et al.* showed isolated teres minor denervation is not uncommon in asymptomatic patients undergoing routine shoulder MR imaging, which may be due to history of surgical intervention, rotator cuff trauma or instability that has likely caused stretching of the posterior branch of the axillary nerve.

Musculocutaneous nerve

The musculocutaneous nerve (MCN) is a mixed nerve that arises from the lateral cord of the brachial plexus; it receives fibers from the C5–C7 nerve roots and provides motor innervation to the coracobrachialis, biceps brachii, and brachialis muscles, as well as sensory innervation to the lateral aspect of the forearm. At the axilla, the
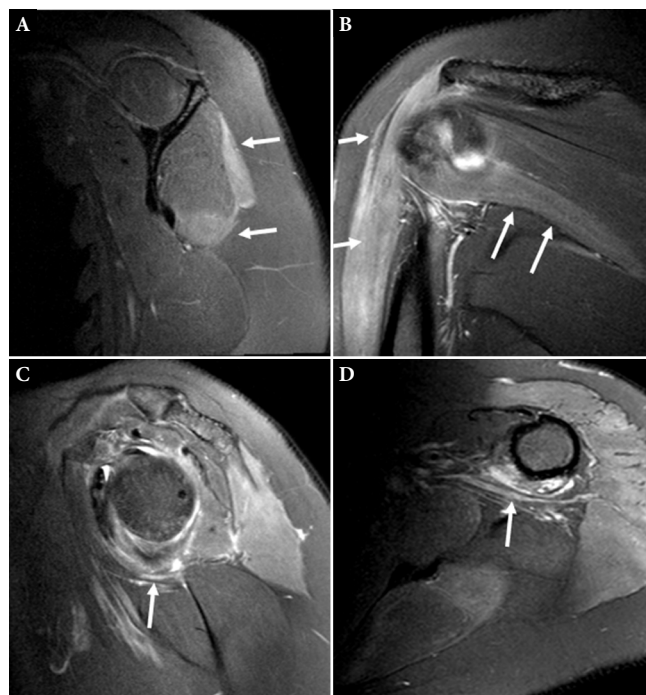

Fig. 3. *46-year-old female with recent right shoulder dislocation and subsequent shoulder weakness and numbness over the deltoid muscle.* **A.** *Sagittal and* **B.** *coronal T2-weighted (T2W) fat-suppressed (FS) MR images of the right shoulder demonstrate diffuse edema within the deltoid and teres minor muscles consistent with denervation. Additional* **C.** *sagittal and* **D.** *axial T2W MR images demonstrate fascicular thickening and increase signal of the axillary nerve consistent with axillary neuropathy*

nerve is lateral to the axillary artery and the median nerve. The nerve then travels anteriorly to pierce the coracobrachialis muscle, after which it descends between the biceps brachii and brachialis muscles to terminate as the lateral cutaneous nerve of the forearm[20]. Similar to other nerves, the MCN can be damaged by trauma, such as fractures or lacerations, or tumors. The MCN can be injured anywhere along its course, but it is most commonly injured as it traverses the coracobrachialis muscle, which can occur due to hypertrophy of the muscle resulting from repetitive strain[21,22]. Additionally, cases of MCN neuropathy have been reported following anterior humeral dislocations[23]. US can identify the MCN along its course from the axilla to the elbow, in addition to the lateral antebrachial cutaneous nerve. Furthermore, US has proven valuable in detecting a diverse range of abnormalities, such as neuromas and traumatic injuries to the nerve[24]. US of the MCN can be performed with the extremity in mild abduction and the hand in supination or the arm in abduction with the hand in supination positioned behind the head (Fig. 4). Similar to other neuropathies, MRN can help detect signal and size changes of the nerve along with target muscle denervation.

Lateral antebrachial cutaneous nerve (LACN)

In the cubital fossa, the MCN courses lateral to the biceps brachii tendon, giving rise to the LACN, a pure sensory nerve innervating the lateral aspect of the forearm. The LACN emerges at the lateral border of the biceps brachii muscle and courses along the lateral border of its tendon adjacent to the cephalic vein. It pierces the antebrachial fascia at a variable location and then courses subcutaneously distally. Its superficial location makes the nerve prone to compressive injury, traction and iatrogenic injuries. Frequent causes of neuropathy of the LACN include repetitive and forceful pronation in athletes involved in throwing sports, compression due to tourniquet use, phlebotomy in the antecubital fossa, incorrectly placed blood pressure cuffs, and positioning during general anesthesia[25]. The nerve can be also injured secondary to rupture of the distal biceps brachii tendon. Additionally, because of its superficial location, the LACN can be injured by penetrating trauma (Fig. 5). Clinically, it presents with pain and dysesthesia of the lateral aspect of the forearm, which can extend anywhere from the elbow to the wrist.
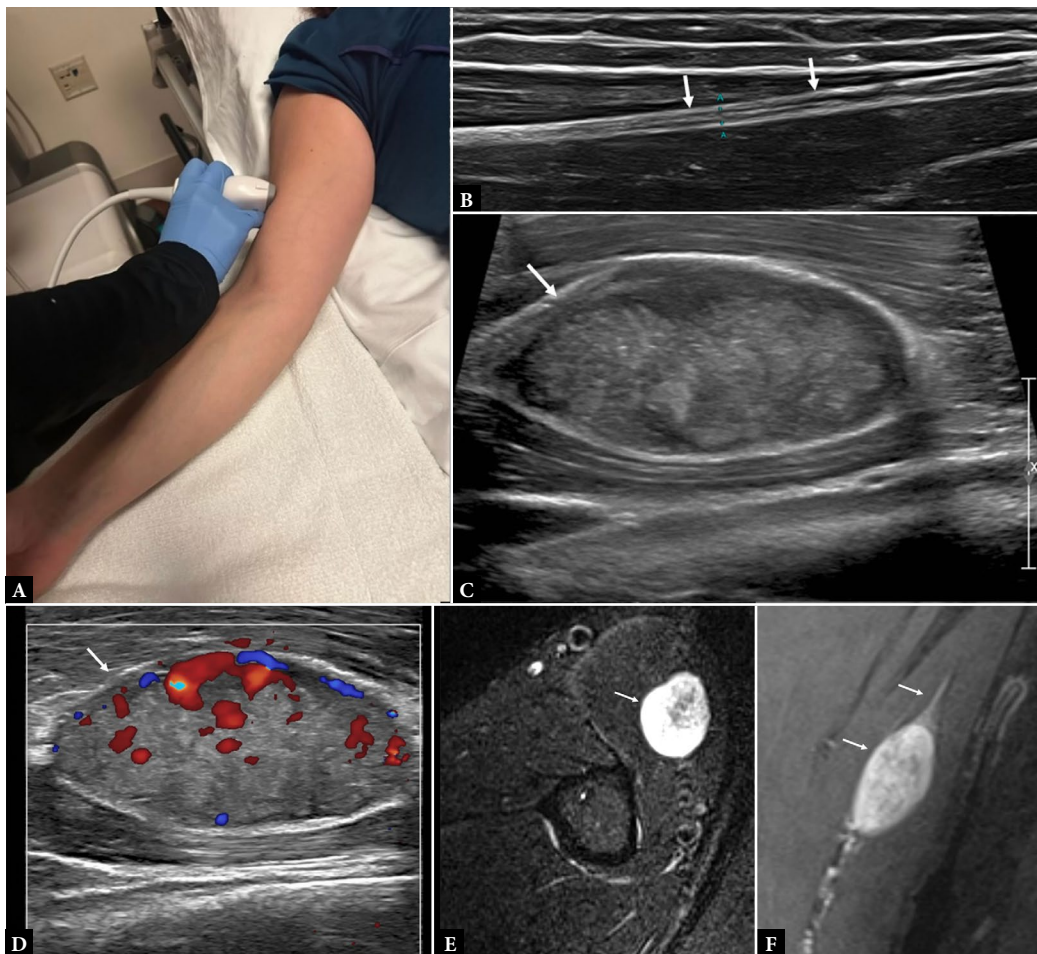

Fig. 4. *Imaging of the musculocutaneous nerve using 24 MHz linear transducer. **A.** Photograph of the right arm demonstrates the probe position for short-axis US imaging of the musculocutaneous nerve in the upper arm. **B.** Long-axis grayscale ultrasound (US) image of the musculocutaneous nerve demonstrates a uniform nerve caliber with normal nerve echogenicity and fascicular echotexture (arrows). **C.** Long-axis grayscale US image in a 37-year-old male with palpable abnormality in the arm and occasional pain. There is an ovoid echogenic lesion (arrow) along the expected course of the musculocutaneous nerve splaying the biceps and brachialis muscles. **D.** Long-axis color Doppler US image of the lesion demonstrates increased Doppler flow (arrow), consistent with a moderately vascular solid lesion. MR neurography images of the same patient through the mass, including **E.** axial T2W FS and **F.** coronal T1-weighted (T1W) FS post contrast images confirm the location of the lesion (arrow) along the musculocutaneous nerve course with a proximal tail sign (upper arrow on F). Pathology showed a schwannoma*
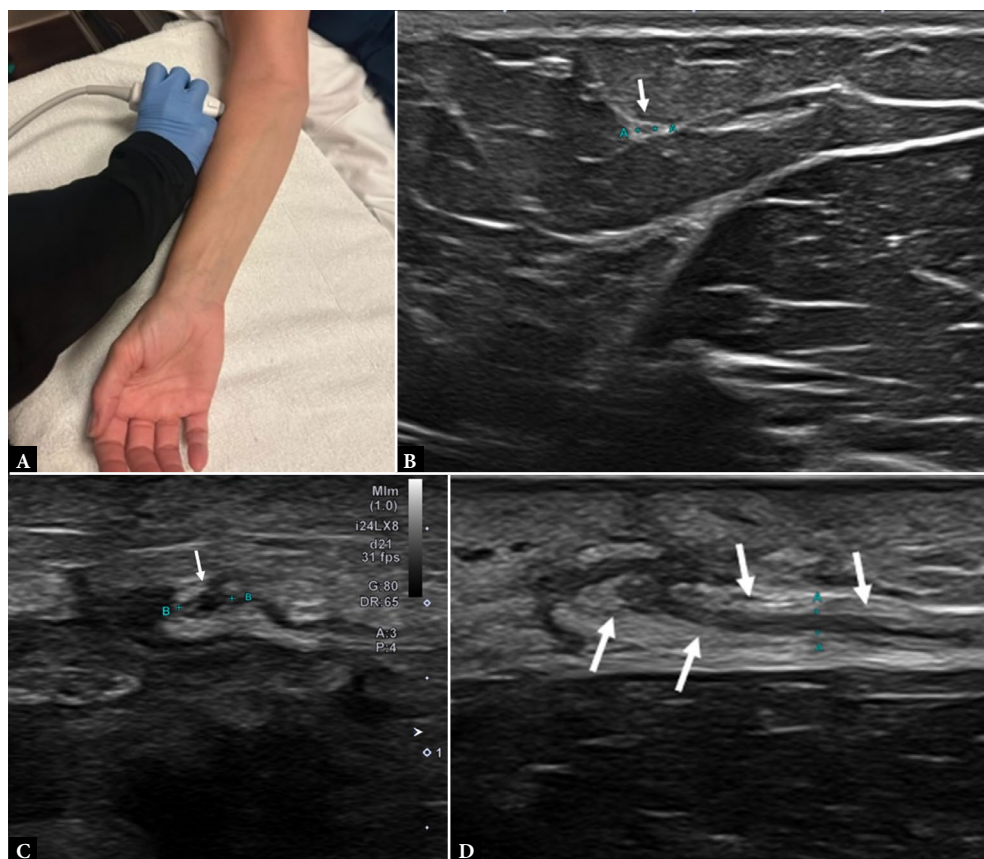
Fig. 5. *Imaging of the lateral antebrachial cutaneous nerve using 24 MHz linear transducer.* **A.** *Photograph of the right hand demonstrates the probe position for short-axis US imaging of the lateral antebrachial cutaneous nerve.* **B.** *Short-axis grayscale US image of the lateral antebrachial cutaneous nerve demonstrates a uniform nerve caliber with normal nerve echogenicity (arrow).* **C.** *Short-axis grayscale US image in a 42-year-old male with history of dog bite of the lateral elbow and numbness in the distribution of the lateral antebrachial cutaneous nerve demonstrates thickening and hypoechogenicity of the nerve at the site of the penetrating injury (arrow).* **D.** *Long-axis grayscale US image demonstrates interruption of the nerve (arrows) at the level of the scar consistent with traumatic nerve transection*

In order to image the LACN, the US transducer should be positioned on the crease of the elbow; in this position, the short axis of the LACN can be visualized on the lateral side of the biceps brachii tendon. The cephalic vein is adjacent to the LACN and can be easily identified[26]. Similar to other nerves, enlargement and increased echogenicity on US and increased T2 signal and enlargement of the nerve are seen in case of neuropathy.

Ulnar nerve

The ulnar nerve originates from the medial cord of the brachial plexus from the C8 and T1 nerve roots. In the arm, it traverses the medial intermuscular septum (arcade of Struthers) and courses posteriorly along the medial aspect of the triceps muscle until it passes distally through the cubital tunnel at the elbow. The floor of the cubital tunnel is formed by the joint capsule and the posterior band of the ulnar collateral ligament; the roof is formed by the retinaculum between the olecranon and the medial epicondyle (Osborne ligament), and distally, the aponeurosis joins both heads of the flexor carpi ulnaris muscle[27]. During elbow flexion, there is decreased cubital tunnel volume and ulnar nerve cross-sectional area. In the forearm, the ulnar nerve pierces the flexor carpi ulnaris fascia and descends beside the ulna toward the wrist, where it enters the hand via the ulnar canal (also known as Guyon's canal). As a result, the most common sites of entrapment are at the cubital tunnel and at the ulnar canal (Fig. 6)[28]. The ulnar nerve innervates the flexor carpi ulnaris muscle and the ulnar side of the flexor digitorum profundus muscle, the hypothenar muscles, the dorsal and palmar interosseous muscles of the hand, the adductor pollicis muscle, and the flexor digitorum profundus muscle. It provides sensation to the small finger, the radial half of the ring finger, and the ulnar side of the hand and wrist with known anatomic variations.

Cubital tunnel syndrome

The cubital tunnel is the second most common location of compressive neuropathy of the upper limb after carpal tunnel syndrome. Cubital tunnel syndrome clinically presents with elbow pain and numbness, tingling and dysesthesia in forearm, the small finger and ulnar half of the ring finger, and if left untreated, it may result in weakness and atrophy of the flexor carpi ulnaris muscle, the ulnar half of the flexor digitorum profundus muscle, hypothenar muscles, adductor pollicis muscle, fourth and fifth lumbrical muscles, and all of the interosseous muscles[29]. It is usually caused by compression of the ulnar nerve at one of the three segments of the cubital tunnel: the retrocondylar groove, the humeroulnar arcade, and the deep flexor/pronator apo-
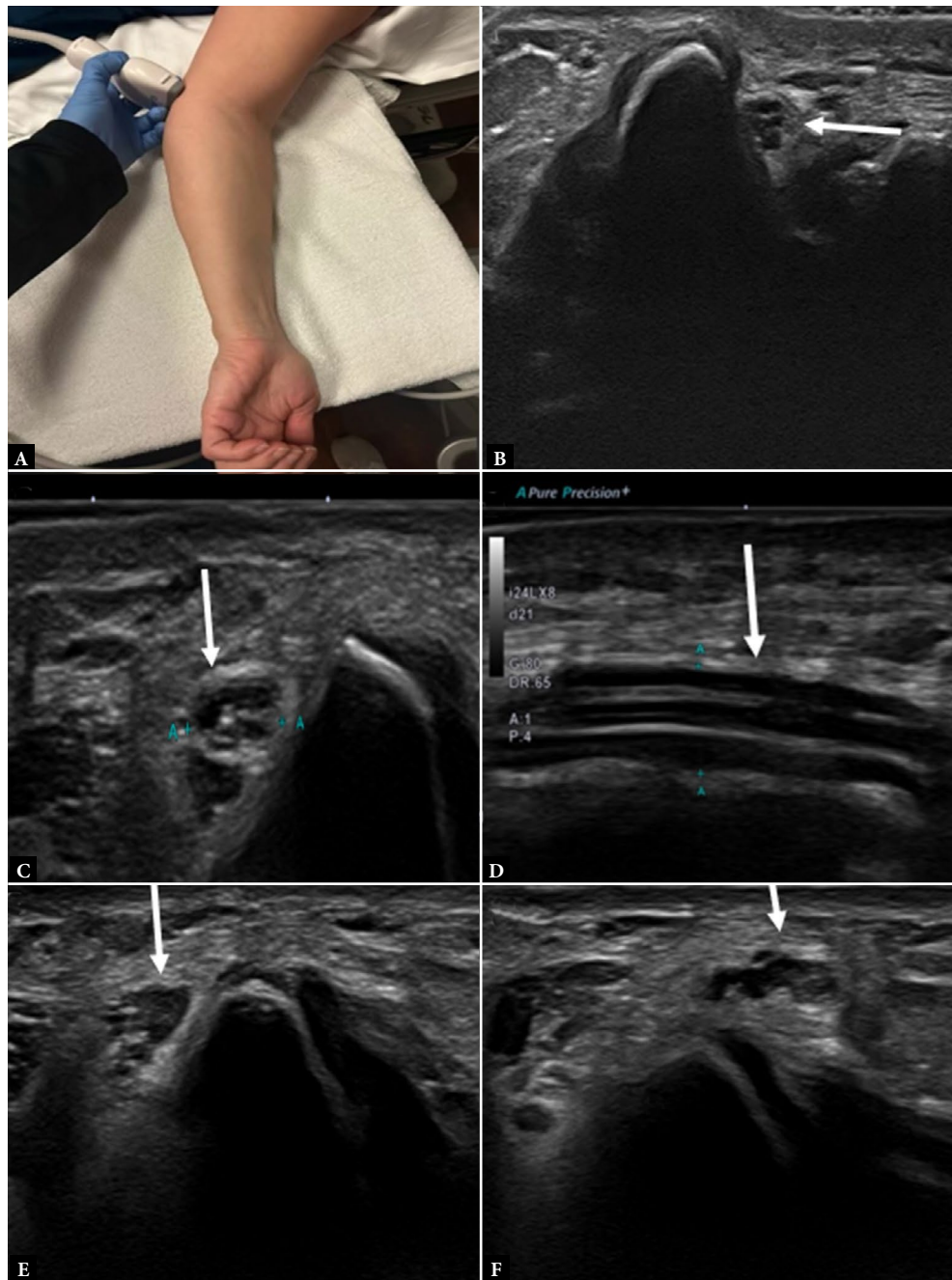
Fig. 6. *Imaging of the ulnar nerve using 24 MHz linear transducer.* **A.** *Demonstrates the probe position for short-axis US imaging the ulnar nerve in the cubital tunnel.* **B.** *Transverse grayscale US image of the ulnar nerve in the cubital tunnel demonstrates normal "honeycomb" appearance of the nerve in the short axis (arrow).* **C.** *Short-axis and* **D.** *Long-axis US images of the ulnar nerve in the cubital tunnel in a 45-year-old male with numbness and tingling in the hand along the ulnar nerve distribution, show fascicular thickening of the nerve (arrows). Dynamic maneuvers with elbow flexion and extension were performed to assess the ulnar nerve position.* **E.** *Short-axis US image of the ulnar nerve with the elbow extended shows the nerve in the normal position within the cubital tunnel posterior to the medial humeral epicondyle (arrow).* **F.** *Short-axis US image of the ulnar nerve in the same location with the elbow flexed depicts displacement of the ulnar nerve anterior to the medial humeral epicondyle (arrow)*

neurosis[30]. Cubital tunnel syndrome is divided into primary and secondary forms[31]; the primary form involves cases in which there are no bony changes or space-occupying lesions along its course, and it may result from nerve friction, from luxation of the ulnar nerve during movement of the joint, nerve traction over the medial humeral epicondyle seen with prolonged elbow flexion, a hypertrophied or dislocated medial head of the triceps muscle or the presence of an accessory anconeus epitrochlearis muscle. Of note, muscular anatomic variants are frequently present in asymptomatic subjects and may be associated with higher rates of ulnar neuropathy without necessarily causing clinical symptoms. The secondary form includes the presence of space-occupying lesions, such as lipomas or ganglion cysts, malunited distal humeral fractures causing bone deformities, exostoses and osteoarthritis with osteophytes, causing extrinsic nerve compression[31].

US imaging is usually done with both static and dynamic techniques. It can be performed with the elbow positioned on the examination table and elbow in extension and slight lateral rotation or with the elbow flexed to 90 degrees and the hand lying flat on the examination table. The nerve can be initially identified along the posteromedial aspect of the elbow, between the olecranon and the medial humeral epicondyle.

Characteristic static sonographic findings of neuropathy include swelling of the nerve proximally with flattening at the site of compression, loss of the normal fascicular pattern, and increased vascularity on Doppler interrogation. There is no universal agreement on the cut-off of the maximal cross-sectional area to diagnose cubital tunnel syndrome, however a cutoff of 10 mm^2 on US is considered to be diagnostic with a sensitivity of 85% and specificity of 91%[26,32]. Dynamic US evaluation should be done during elbow flexion and extension, which allows real-time examination of nerve stability within the retroepicondylar groove and can be compared to the contralateral side at the same time. It can detect reduced nerve mobility, or anterior nerve subluxation or frank dislocation from the cubital tunnel over the medial humeral epicondyle during active elbow flexion (Video 1). In cases in which the neuropathy is related to nerve luxation or traction during elbow flexion, the nerve may be most thickened with loss of the fascicular echotexture at the level of the medial humeral epicondyle, which tapers to a normal caliber gradually cranially and caudally.

Guyon's canal syndrome

At the wrist, the ulnar nerve travels within Guyon's canal. Proximal to the canal, the nerve gives a dorsal branch that innervates the dorsal aspect of the small finger and the ulnar half of the ring finger, and a smaller palmar branch that innervates the hypothenar eminence; however, this branch is too small to be routinely evaluated on imaging. Within Guyon's canal, the nerve divides into two terminal branches: a superficial branch that travels between the palmar aponeurosis and the hypothenar muscles, provides sensory innervation and gives a small motor branch for the palmaris brevis muscle; and a deep branch that provides motor innervation to the hypothenar muscles[33]. The deep branch distal to the canal innervates the intrinsic hand muscles supplied by the ulnar nerve, including the interosseous, third and fourth lumbrical, adductor pollicis and the flexor pollicis brevis deep head muscles. Guyon's canal is a fibro-osseous tunnel at the ulnar border of the palmar aspect of the wrist. It contains the ulnar nerve and artery as they pass through to the hand. It is bordered by the volar carpal ligament, which forms the roof; the transverse carpal ligament, which forms the floor; the hook of hamate, which creates the radial border; and the pisiform, flexor carpi ulnaris tendon and abductor digiti minimi muscle, which make the ulnar border. In contrast to carpal tunnel syndrome, Guyon's canal syndrome is never idiopathic. Most references classify Guyon's canal syndrome into three categories based on the location of compression, symptoms induced, and etiologies. Category 1 occurs proximal to nerve bifurcation and causes primary mixed motor and sensory symptoms. Category 2, which is usually seen distal to the nerve bifurcation, affects the deep terminal motor branch, and causes motor symptoms to all of the previously mentioned muscles except the flexor carpi ulnaris and flexor digitorum profundus muscles. Category 3 occurs distal to the nerve bifurcation, affects the superficial sensory terminal branch of the ulnar nerve and causes sensory symptoms only. It is usually related to vascular causes, like an enlarged thrombosed ulnar vein, thrombosed ulnar artery and ulnar artery pseudoaneurysm[34]. Denervation muscle changes of the hand muscles supplied by the ulnar nerve that spare the flexor carpi ulnaris and ulnar half of the flexor digitorum profundus muscles in the forearm can help to localize a more distal source of ulnar neuropathy when compared to findings of cubital tunnel syndrome. Categories 1 and 2 are usually caused by fractures of the hook of hamate, pisiform, or metacarpal bases with malunion or nonunion, ganglion cysts, lipomas, or other tumors. Additional potential causes of ulnar nerve compression in the hand are accessory muscles, most commonly the accessory abductor digiti minimi, which can be hypertrophied. However, these variants are often present in healthy asymptomatic people, and are frequently bilateral. Sonographic comparison of both sides can be helpful to detect muscle hypertrophy potentially contributing to compressive neuropathy[35].

US depicts the ulnar nerve in Guyon's canal and its terminal branches well to the level of the hook of hamate, but these branches are more difficult to visualize distally, particularly when there is muscle fatty infiltration. CT examination is often helpful to detect fractures in cases of trauma or osteophytes in cases of osteoarthritis, and CT or MR angiography may be helpful in cases where vascular abnormalities are suspected. High-resolution US can be used to measure the cross-sectional area of the nerve within Guyon's canal, which can be compared with the contralateral asymptomatic nerve to detect subtle nerve swelling.

High-resolution MRN of the wrist or proximal hand easily depicts the ulnar nerve as it passes through Guyon's canal, and it can assess whether there is denervation edema or atrophy of the muscles supplied by the nerve. Magic angle artifact, often seen on MRN pulse sequences with low echo times, is a pitfall caused by the curvature of the ulnar nerve in the wrist that can mimic nerve pathology. However, in cases of nerve signal abnormality related to magic angle artifact, the nerve should remain normal in caliber, and there should not be associated space-occupying lesions or muscle denervation changes.

Radial nerve

The radial nerve is one of the two terminal branches of the posterior cord of the brachial plexus, arising from the C5-T1 nerve roots, and it descends within the upper arm along the posterior part of the humerus through a depression called the spiral groove[36]. It wraps around the distal humerus and courses along the lateral aspect of the humeral diaphysis until it reaches the radial tunnel. The radial tunnel is about 5 cm in length and located between the radiocapitellar joint proximally and the proximal edge of the supinator muscle distally. The tunnel is bounded laterally by the brachioradialis, and extensor carpi radialis longus and brevis muscles, and medially by the brachialis muscle. Approximately 3 cm distal to the lateral humeral epicondyle, the radial nerve divides into two branches, the superficial sensory radial nerve and deep motor branch, also called the posterior interosseous nerve (PIN), which passes between the two heads of the supinator muscle. The level of division of the radial nerve however can be variable. The cranial border of the superficial head of the supinator muscle is composed of a fibrous arch called the arcade of Fröhse. Distally, the PIN splits into superficial and deep branches and innervates the dorsal compartment of the forearm[37]. The superficial branch of the radial nerve courses under the brachioradialis muscle between the heads of

the extensor carpi radialis longus and the brachioradialis muscles to innervate the dorsoradial hand (thumb and index finger)[38]. The radial nerve can be entrapped anywhere along its course, with possible involvement above or at the elbow (Fig. 7).

Injuries of the radial nerve above the elbow

Radial nerve injuries are common in humeral shaft fractures, especially spiral fractures of the distal third of the diaphysis[39,40]. Injuries may result in a wide range of symptoms depending on the severity of injuries, ranging from simple contusion to complete transection. Other causes include abnormal bone formation, deep intramuscular injections, prolonged compression or immobilization, among others[41].

Due to its size and superficial location, the radial nerve is usually easily seen on US and MRN. The PIN is best initially identified at the level of the supinator muscle and the radial neck, where the nerve courses in the fascial plane between the deep and superficial heads of the supinator muscle. This muscle is easy to identify, since it distinctively wraps around the radial neck, and, unlike most other muscles in the forearm, its fibers are oriented transverse to the long axis of the upper extremity. With involvement of the radial nerve at or just above the elbow, active elbow extension is usually intact, because of the branch of the radial nerve supplying the triceps brachii muscle usually arises more proximally.

Injuries of the radial nerve at the elbow: radial tunnel syndrome (RTS) and posterior interosseous nerve syndrome (PINS)

Both RTS and PINS refer to the compression of the deep motor branch of the PIN at the level of the elbow within the radial tunnel. The main difference is the severity of compression and the clinical presentation, as RTS can result in sensory symptoms such as pain in the lateral elbow and forearm without motor deficit, which may be confused clinically with lateral epicondylitis. On the other hand, PINS presents with pain and motor weakness involving finger extension with preserved wrist extension[42]. In this condition, the wrist extensors are not affected since the brachioradialis and the extensor carpi radialis longus muscles responsible for wrist extension are both supplied by the radial nerve above the elbow[43]. Electromyography (EMG) evaluation is usually normal in the case of radial tunnel syndrome, but positive in the case of PINS. As with other cases of neuropathy, causes include extrinsic compression or nerve injury from repetitive microtrauma. The most common site of PIN injury is compression at the arcade of Fröhse. Other causes include nerve compression in the lateral elbow at the level of the radial head secondary to inflammatory arthropathy or fibrous adhesion anterior to the radiocapitellar joint, compression by an arcade of branches of the recurrent radial artery at the radial neck and a fibrous edge of the medial proximal extensor carpi radialis brevis (leash of Henry)[44].

On US, signs of neuropathy, including hypoechoic swelling of the PIN, are observed proximal to the site of compression (Fig. 8). Associated findings, like hyperechoic thickening of the arcade of Fröhse, radiocapitellar ganglion cysts, soft tissue masses and bicipitoradial bursitis, may suggest the cause of compressive neuropathy[45]. Supinator muscle fatty atrophy is a common finding of PINS on both US
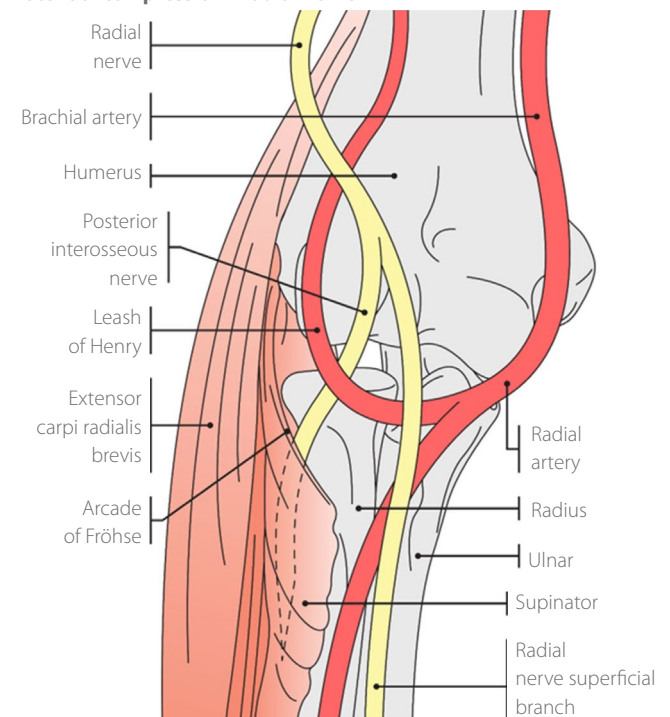
Potential compression – radial nerve

Fig. 7. *Diagram showing the common sites of the radial nerve and posterior interosseous nerve compression*

and MRN, although MRN may help detect earlier stages of PINS if there is reversible muscle edema without muscle atrophy.

Superficial radial neuropathy

This entity, also known as Wartenberg's syndrome or cheiralgia paresthetica, usually results from entrapment of the superficial branch of the radial nerve. The distal segment of this nerve is located superficially and radially in the distal forearm and wrist and divides into medial and lateral branches. Given its superficial location, it is susceptible to injuries. Clinically, this condition presents with purely sensory symptoms like pain and paresthesia on the dorsal and radial sides of the hand and can mimic de Quervain's tenosynovitis. Superficial radial neuropathy is most commonly posttraumatic due to the superficial location of the nerve, and can result from penetrating wounds, tight watch bands or handcuffs, distal radius fracture fragments, and steroid injections for de Quervain's tenosynovitis, among other entities[46]. In addition, some movements like hyperpronation can compress the nerve between the extensor carpi radialis longus and the brachioradialis muscles; occasionally, superficial radial neuropathy related to hyperpronation can be related to a fibrous fascia between these two muscles[47].

On imaging, the superficial branch of the radial nerve is often normally closely related to the first extensor compartment tendons in the distal forearm near the wrist and may cross over the tendons[48]. US of abnormal nerves usually shows loss of the normal fascicular pattern with swelling and increased hyperemia on Doppler imaging, and MRN can show thickening and increased signal of the nerve on fluid-sensitive sequences with variable enhancement on the post contrast sequences.
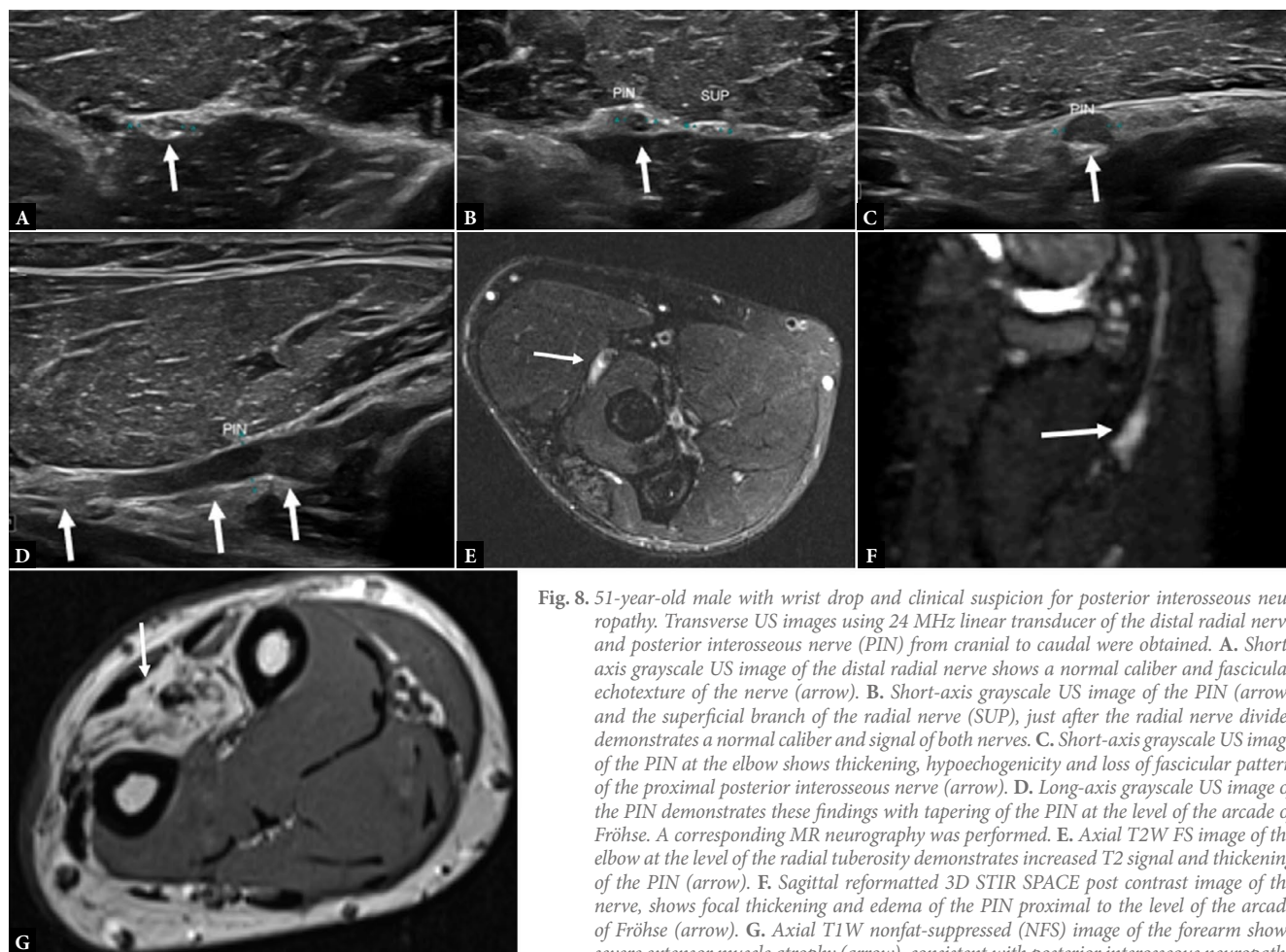
Fig. 8. *51-year-old male with wrist drop and clinical suspicion for posterior interosseous neuropathy. Transverse US images using 24 MHz linear transducer of the distal radial nerve and posterior interosseous nerve (PIN) from cranial to caudal were obtained. **A.** Short-axis grayscale US image of the distal radial nerve shows a normal caliber and fascicular echotexture of the nerve (arrow). **B.** Short-axis grayscale US image of the PIN (arrow) and the superficial branch of the radial nerve (SUP), just after the radial nerve divides demonstrates a normal caliber and signal of both nerves. **C.** Short-axis grayscale US image of the PIN at the elbow shows thickening, hypoechogenicity and loss of fascicular pattern of the proximal posterior interosseous nerve (arrow). **D.** Long-axis grayscale US image of the PIN demonstrates these findings with tapering of the PIN at the level of the arcade of Fröhse. A corresponding MR neurography was performed. **E.** Axial T2W FS image of the elbow at the level of the radial tuberosity demonstrates increased T2 signal and thickening of the PIN (arrow). **F.** Sagittal reformatted 3D STIR SPACE post contrast image of the nerve, shows focal thickening and edema of the PIN proximal to the level of the arcade of Fröhse (arrow). **G.** Axial T1W nonfat-suppressed (NFS) image of the forearm shows severe extensor muscle atrophy (arrow), consistent with posterior interosseous neuropathy*

Median nerve

The median nerve is a mixed sensory and motor nerve, formed by the confluence of the medial and lateral cords of the brachial plexus with contributions from the C5-T1 nerve roots. It descends in the upper arm along the medial side of the brachial artery, and then crosses the artery to become lateral to the artery more distally. At the elbow, it courses under the bicipital aponeurosis, medial to the biceps brachii tendon and the brachial artery, and enters the forearm between the two heads of the pronator teres muscle, where it gives rise to the anterior interosseous nerve (AIN) (Fig. 9)[49]. It passes deep to the sublime bridge, a fibrous sheath formed by the two heads of the flexor digitorum superficialis, and passes distally between the flexor digitorum superficialis and flexor digitorum profundus muscles, giving rise to the palmar cutaneous branch before it enters the carpal tunnel[50].

Pronator teres syndrome

Pronator teres syndrome refers to all causes of compression of the median nerve proximal to the AIN, not just the entrapment between the two heads of the pronator teres[50]. Clinically, it can present similarly to carpal tunnel syndrome, with numbness and tingling of the thumb, the index and long fingers, and the radial aspect of the ring finger. However, the presence of pain in the forearm and a negative Tinel sign and Phalen maneuver suggest pronator teres syndrome[51]. Motor symptoms are variable. The nerve may be compressed between the humeral and ulnar heads of the pronator teres muscle, which is usually seen in patients with repetitive pronation-supination; under the bicipital aponeurosis, also called the lacertus fibrosus; at the ligament of Struthers, which runs from the supracondylar process of the humerus, which is an anatomic variant that presents in only 1% of the population and is also called an avian spur, and the medial epicondyle; or by an accessory head of the flexor pollicis longus muscle[52,53]. Lateral humeral or elbow radiographs may be helpful to identify supracondylar processes.

On transverse imaging, the median nerve is easiest to initially identify in the volar distal forearm and wrist as a superficial structure entering the carpal tunnel, and it can be traced proximally in the forearm between the two heads of the pronator teres muscle. For cases of pronator teres syndrome, in addition to the direct signs of neuropathy and compressive space-occupying lesions, radiologists should focus on the echotexture of the pronator teres muscle to assess for hypertrophy, fibrosis or any other signs of muscle denervation or any lesions responsible for compression. Comparison with the contralateral side may be helpful to detect subtle asymmetry or the presence of anatomical variants, like the supracondylar process[54].

Anterior interosseous nerve syndrome (AINS)

AINS usually results from the compression of the AIN, and presents with acute pain in the proximal forearm followed by weakness on flexion of the thumb at its interphalangeal joint and the index finger at its distal interphalangeal joint. On physical examination, patients are unable to bring the tips of the index finger and thumb together in the shape of an "O", which is called a positive Kiloh-Nevin sign[55]. AINS could result from nerve compression due to repetitive elbow flexion and pronation, compression from a fibrous band of the superficial head of the pronator teres, an aberrant course of the radial artery, or thrombosed anterior interosseous vessels. Noncompressive causes, such as interstitial neuritis, can also be considered[56]. Usually, EMG studies are normal in AINS, and direct signs of neuropathy are inconclusive on imaging due to the small size of the nerve[57]. On MRN, fat-suppressed, fluid-sensitive images show diffuse edema of denervated muscles, especially the pronator quadratus muscle, while chronic denervation may result in muscle atrophy or fatty infiltration on T1W imaging (Fig. 10)[58]. Finally, physicians should be aware of important upper limb anatomical nerve variations, like the Martin-Gruber anastomosis, which in cases of AINS can cause denervation edema in muscles not classically innervated by the AIN due to its anastomosis with the ulnar nerve[59].
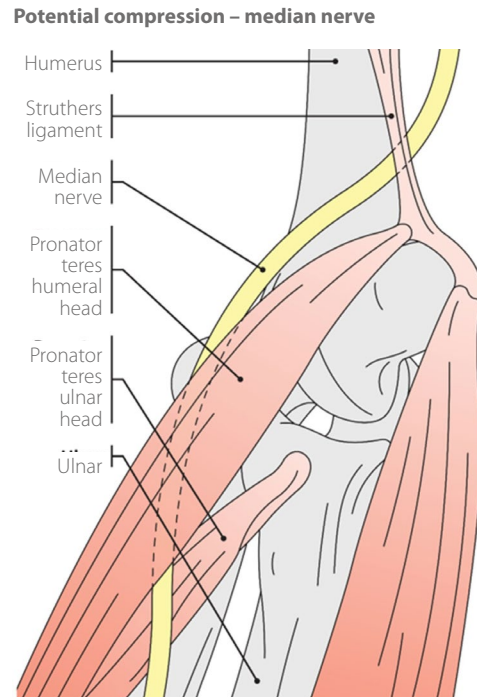

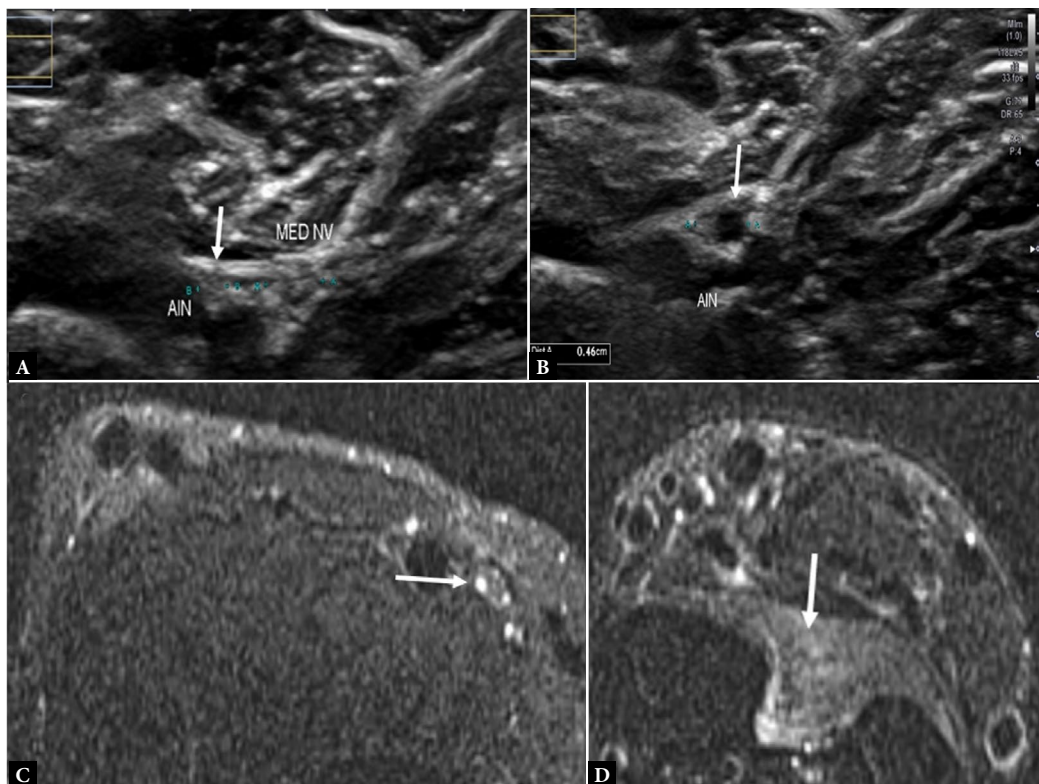**Fig. 9.** *Diagram showing the common sites of median nerve compression about the elbow*

Fig. 10. *37-year-old male with arm pain and weakness with clinical and EMG concern for anterior interosseous neuropathy. Transverse US images of the anterior interosseous nerve (AIN) using 18 MHz linear transducer in the forearm were obtained. **A.** Short-axis grayscale US image in the mid forearm shows the normal caliber and echotexture of the AIN (between the calipers marked "B"), which has a fine fasciculated appearance (arrow). The median nerve (between calipers marked "A") is larger at this level but has similar echotexture and echogenicity. **B.** A more distal forearm grayscale US image of the AIN demonstrates a thickened, hypoechoic appearance of the AIN (arrow). **C.** MR neurography axial STIR image of the mid forearm before the AIN divides from the median nerve demonstrates increased median nerve fascicular edema involving its fibers that contribute to the AIN. **D.** More distal forearm axial STIR MR image demonstrates diffuse pronator quadratus muscle edema felt to be related to denervation*

Carpal tunnel syndrome (CTS)

CTS is the most common upper extremity entrapment neuropathy. The carpal tunnel is an osteofibrous canal in the volar wrist, bounded by the carpal bones forming the floor; the transverse carpal ligament, also called flexor retinaculum, forming the roof; the pisiform ulnarly; and the scaphoid tubercle radially. It contains the flexor tendons and the median nerve, which is usually the most superficial structure. Anything that decreases the space inside the carpal tunnel can cause median nerve compression. This includes compressive neuropathy, which includes multiple causes, like bone fractures, hematoma, soft tissue and nerve tumors, flexor bursitis, volar wrist synovitis, joint effusion and some anatomical variants that may cause compression of the median nerve[60,61]. There are multiple systemic conditions associated with CTS, including pregnancy, kidney failure, diabetes, hypothyroidism, and the use of oral contraceptives[62] although the cause can remain indeterminate. Usually, patients initially present with sensory symptoms, while motor symptoms are delayed. They commonly experience pain and paresthesias in the palmar aspect of the thumb, index and long fingers and radial half of the ring finger, and in more advanced cases, weakness of thumb abduction and opposition, reduced finger grip and thenar muscle atrophy[63].

On US, which is the gold standard imaging test for CTS, the median nerve is visualized as a hypoechoic, fasciculated, oval structure with similarly sized hypoechoic fascicles when seen in the short axis, and

US has similar sensitivities and specificities as EMG studies in diagnosing CTS but can better characterize the nerve and surrounding anatomical structures[64]. The diagnosis of CTS on US is based on measuring the cross-sectional area of the median nerve by tracing the hypoechoic nerve, excluding the echogenic perineurium. Numerous studies have examined the cross-sectional area of the nerve, yielding variable findings. However, the generally accepted upper normal limit is 11–12 mm^2. Another method for assessing nerve size involves measuring the cross-sectional area at two different locations: the carpal tunnel, where the nerve is largest, and the proximal margin of the pronator quadratus muscle. A difference of more than 2 mm^2 between these two levels has high sensitivity and specificity for the diagnosis of CTS (Fig. 11). If the nerve is bifid, each part must be measured separately, and the sum of the measurements used. A pathologic condition is indicated if the cross-sectional area difference exceeds 4 mm^2, and the upper normal limit for cross-sectional area is also around 11–12 mm$^{2[65,66]}$. Although, using the cross-sectional area difference is more reliable in diagnosing neuropathy compared to using the cross-sectional area of the nerve at a specific site with a cut off of 11–12 mm^2, as the nerve might be larger in asymptomatic individuals. A persistent median artery (PMA), which is an anatomic variant representing a remnant of the embryological median artery, occasionally persists into adulthood as a sizeable artery that can be seen accompanying the median nerve. It is often associated with bifid median nerves, and has been reported in up to half of the bifid median nerve cases[67] (Fig. 12). A PMA can contribute
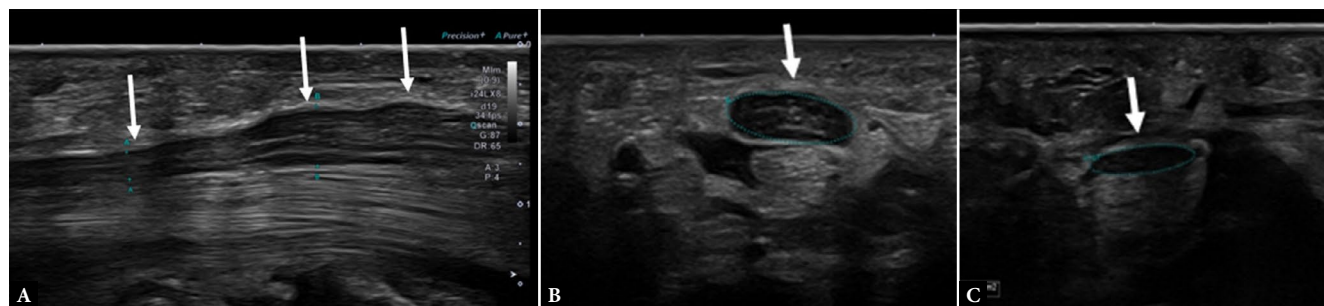

Fig. 11. *50-year-old female with palmar hand numbness in the distribution of the median nerve.* **A.** *Long-axis grayscale US image of the median nerve in the carpal tunnel using 24 MHz linear transducer demonstrated fascicular hypoechogenicity and thickening of the nerve (between calipers marked "B"), and distal narrowing of the nerve (between calipers marked "A").* **B.** *Short-axis grayscale US image of the median nerve at the distal forearm shows a cross sectional area (CSA) of 0.19 cm^2.* **C.** *More distal short-axis grayscale US image of the median nerve within the carpal tunnel shows flattening of the median nerve (arrow) with a CSA of 0.14 cm^2. There is more than 0.02 cm^2 difference between the CSA of the median nerve at the wrist and in the carpal tunnel, suggesting carpal tunnel syndrome*
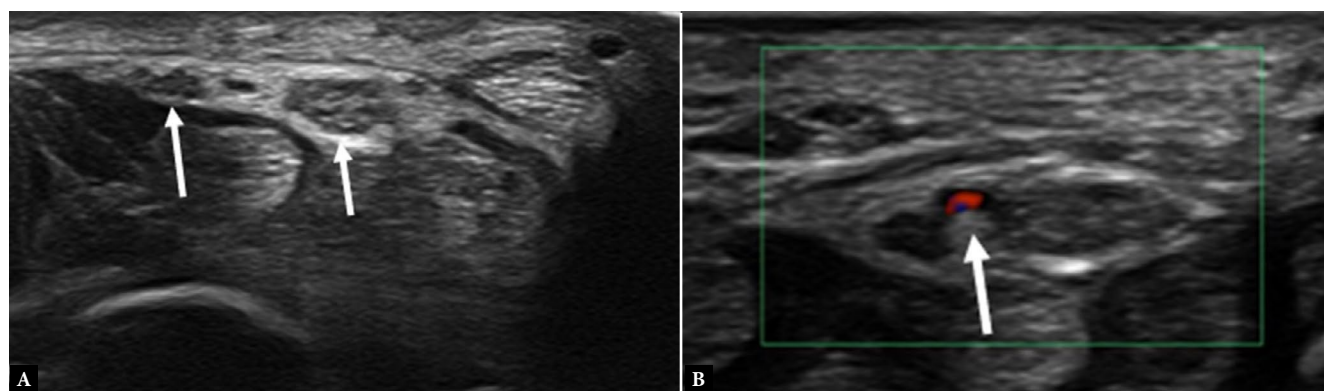

Fig. 12. *56-year-old female with brachial plexus injury presented for upper extremity nerve ultrasound evaluation.* **A.** *Short-axis grayscale ultrasound of the median nerve using 24 MHz linear transducer at the level of the carpal tunnel demonstrated a bifid median nerve (arrow).* **B.** *Short-axis color Doppler US image at more proximal level demonstrated flow within a persistent median artery (arrow)*
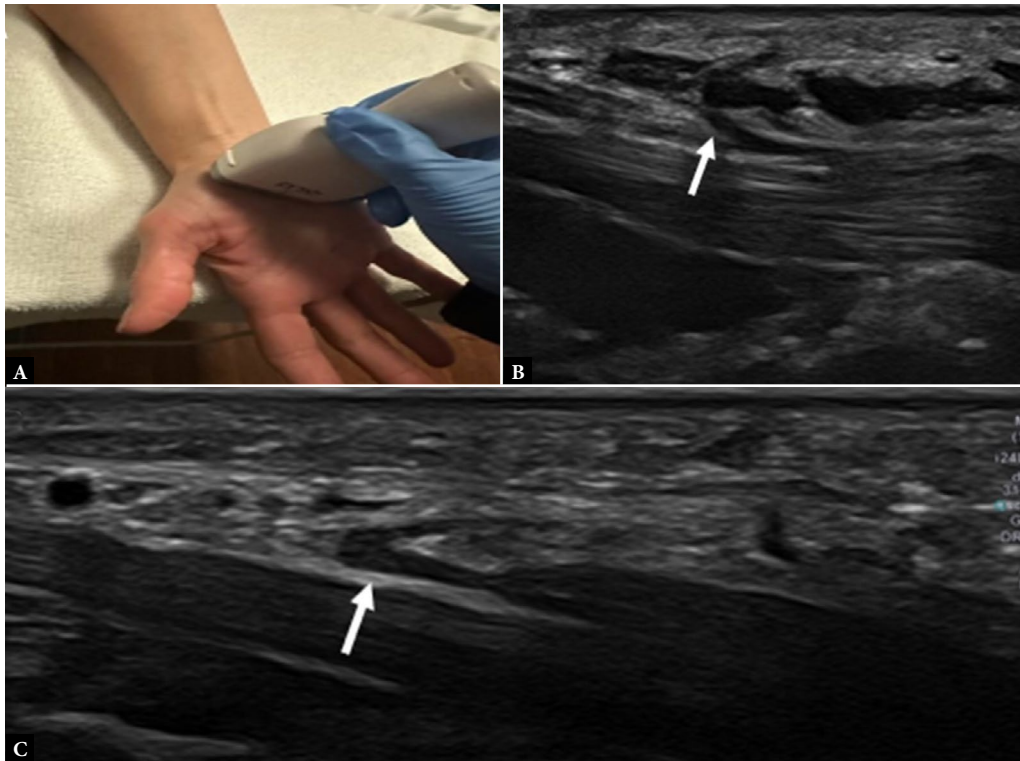
Fig. 13. *Imaging of the recurrent branch of the median nerve using 24 MHz linear transducer. **A.** Photograph of the right hand demonstrating the probe position for imaging the recurrent branch of the median nerve. **B.** Long-axis grayscale US image of the recurrent branch of the median nerve shows the normal sonographic appearance and caliber of the nerve (arrow). **C.** Long-axis grayscale US image in a 63-year-old female with right thumb pain and weakness who was referred for clinical suspicion of median neuropathy demonstrates thickening of the recurrent branch of the median nerve after its origin (arrow), consistent with neuropathy*

to CTS particularly when enlarged or thrombosed[68]. In the scenario of surgical treatment for CTS, the PMA is usually carefully avoided during the surgery because of the risk of vascular compromise of the digits and the increased risk of bleeding when the artery is injured. The PMA should be reported whenever imaging of the carpal tunnel is performed, particularly in a preoperative setting.

Recurrent branch of the median nerve (RBMN)

The RBMN is a pure motor branch that originates from the median nerve and supplies motor innervation to the thenar muscles. Three variants of the course of this nerve to reach the thenar muscles have been described: the extraligamentous type with radial or ulnar branching when the RBMN arises close to the distal end of the transverse carpal ligament and follows a retrograde course to reach the thenar eminence; the subligamentous type, in which the RBMN arises within the carpal tunnel and maintains its course deep to the transverse carpal ligament to reach the thenar eminence; and the transligamentous type, when the nerve arises within the carpal tunnel and then pierces the transverse carpal ligament to reach the thenar eminence[69]. Compression of the recurrent branch can lead to pain, numbness, and weakness in the thenar eminence. Etiologies of RBMN compression include repetitive manual labor, trauma, and space-occupying lesions (Fig. 13). Injuries to this nerve can lead to great dysfunction in the opposability of the thumb, and the nerve has been referred to as the "million-dollar nerve" since iatrogenic RBMN injuries can lead to large malpractice settlements.
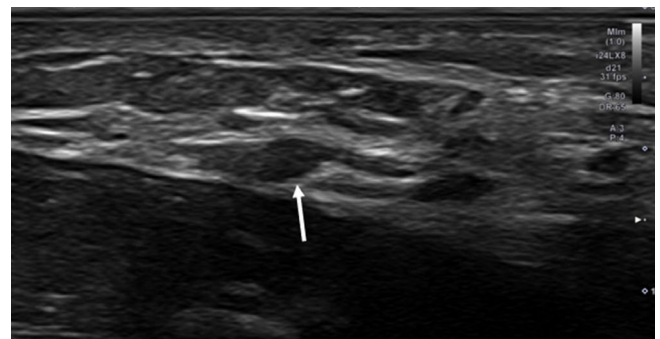

Fig. 14. *45-year-old female with constant numbness of the right thumb and index finger after endoscopic carpal tunnel release performed 2 years ago. A long-axis grayscale US image using 24 MHz linear transducer of the palmar proper digital nerve of the index finger, along the radial aspect of the digit, demonstrates an oval hypoechoic mass-like lesion in continuity with the nerve consistent with neuroma-in-continuity (arrow)*

Digital nerves

The proper digital nerves provide innervation of the digits and are the terminal branches of the radial, median, and ulnar nerves beyond the carpal tunnel and the Guyon's canal[70]. Pathology of the digital nerves is termed digitalgia paresthetica. It is most commonly posttraumatic, given the superficial location of the nerves, and can be caused by penetrating and non-penetrating injuries. Other etiologies include inflammatory, infectious or tumoral causes. Digital

amputation can lead to stump neuromas, which can be painful[71]. Perineural fibrosis of the ulnar proper digital nerve of the thumb has been reported in bowlers and has been named "bowler's thumb". This condition has also been reported in baseball players and is thought to be secondary to repetitive valgus microtrauma that results in nerve traction[72]. The imaging appearance of digital neuropathy is similar to other nerves (Fig. 14). Imaging of digital nerves can be more challenging given their small sizes, and US is often the first-line modality given its higher spatial resolution. A hockey stick US transducer may be preferred to use whenever possible due to its small footprint and the small curved skin surfaces around the base of the thumb. MRN should be adapted to imaging digital nerve by using small coils, small field-of-view, and high-resolution sequences.

Conclusion

Continued advances in diagnostic imaging techniques have resulted in improvements in detecting and characterizing peripheral nerve abnormalities, which has allowed diagnostic imagers the ability to perceive even smaller nerves and nerve fascicles that were previously not visible. Even though the diagnosis of peripheral neuropathies still relies on clinical assessment and electrodiagnostic studies, advanced imaging studies, such as MRN and US, have become mainstays in determining the distribution of nerve involvement, localizing sites of pathology and potential causes of peripheral neuropathies. US can visualize sites of nerve compression and identify the presence of space-occupying lesions, as well as evaluate for the presence and distribution of muscle atrophy, allowing for comparison to the contralateral side. MRN can also provide detailed anatomical information, which allows better localization and assessment of the extent of the neuropathy. It is becoming increasingly important for radiologists assessing peripheral nerves to have a thorough understanding of routine anatomy and common anatomic variants, the clinical presentations of various peripheral neuropathies, and frequent causes and sites of peripheral nerve injuries.

Conflict of interest

The authors do not report any financial or personal connections with other persons or organizations which might negatively affect the contents of this publication and/or claim authorship rights to this publication.

Author contributions

Original concept of study: AS, SKL, JM, MS, IMO. Writing of manuscript: AS, SKL, JM, MS, IMO. Analysis and interpretation of data: AS, SKL, JM, MS, IMO. Final acceptation of manuscript: AS, SKL, JM, MS, IMO. Collection, recording and/or compilation of data: AS, SKL, JM, MS, IMO. Critical review of manuscript: AS, SKL, JM, MS, IMO.

References

1. Hughes RA: Peripheral neuropathy. BMJ 2002; 324: 466–469. doi: 10.1136/bmj.324.7335.466.

2. Taljanovic M, Omar IM, Hoover KB, Chadaz TS: Musculoskeletal imaging. Oxford University Press 2019.

3. Azhary H, Farooq MU, Bhanushali M, Majid A, Kassab MY: Peripheral neuropathy: differential diagnosis and management. Am Fam Physician 2010; 81: 887–892.

4. Franklin GM, Friedman AS: Work-related carpal tunnel syndrome: diagnosis and treatment guideline. Phys Med Rehabil Clin N Am 2015; 26: 523–537. doi: 10.1016/j.pmr.2015.04.003.

5. Telleman JA, Grimm A, Goedee S, Visser LH, Zaidman CM: Nerve ultrasound in polyneuropathies. Muscle Nerve 2018; 57: 716–728. doi: 10.1002/mus.26029.

6. Kerasnoudis A, Tsivgoulis G: Nerve ultrasound in peripheral neuropathies: a review. J Neuroimaging 2015; 25: 528–538. doi: 10.1111/jon.12261.

7. Cambon-Binder A: Ulnar neuropathy at the elbow. Orthop Traumatol Surg Res 2021; 107: 102754. doi: 10.1016/j.otsr.2020.102754.

8. Sehmbi H, Madjdpour C, Shah UJ, Chin KJ: Ultrasound guided distal peripheral nerve block of the upper limb: a technical review. J Anaesthesiol Clin Pharmacol 2015; 31: 296–307. doi: 10.4103/0970-9185.161654.

9. Youngner JM, Matsuo K, Grant T, Garg A, Samet J, Omar IM: Sonographic evaluation of uncommonly assessed upper extremity peripheral nerves: anatomy, technique, and clinical syndromes. Skeletal Radiol 2019; 48: 57–74. doi: 10.1007/s00256-018-3028-z.

10. Taljanovic MS, Gimber LH, Becker GW, Latt LD, Klauser AS, Melville DM et al.: Shear-wave elastography: basic physics and musculoskeletal applications. Radiographics 2017; 37: 855–870. doi: 10.1148/rg.2017160116.

11. Kantarci F, Ustabasioglu FE, Delil S, Olgun DC, Korkmazer B, Dikici AS et al.: Median nerve stiffness measurement by shear wave elastography: a potential sonographic method in the diagnosis of carpal tunnel syndrome. Eur Radiol 2014; 24: 434–440. doi: 10.1007/s00330-013-3023-7.

12. Chalian M, Behzadi AH, Williams EH, Shores JT, Chhabra A: High-resolution magnetic resonance neurography in upper extremity neuropathy. Neuroimaging Clin N Am 2014; 24: 109–125. doi: 10.1016/j.nic.2013.03.025.

13. Kasper JM, Wadhwa V, Scott KM, Rozen S, Xi Y, Chhabra A: SHINKEI – a novel 3D isotropic MR neurography technique: technical advantages over 3DIRTSE-based imaging. Eur Radiol 2015; 25: 1672–1677. doi: 10.1007/s00330-014-3552-8.

14. Martín Noguerol T, Barousse R, Gómez Cabrera M, Socolovsky M, Bencardino JT, Luna A: Functional MR neurography in evaluation of peripheral nerve trauma and postsurgical assessment. Radiographics 2019; 39: 427–446. doi: 10.1148/rg.2019180112.

15. Rastogi P, Stewart DA, Lawson RD, Tremblay DM, Smith BJ, Tonkin MA: Cadaveric dissection of the axillary nerve: an investigation of extra-muscular and intra-muscular branching patterns. J Hand Surg Asian Pac Vol 2018; 23: 533–538. doi: 10.1142/s2424835518500546.

16. Nishimura M, Kobayashi M, Hamagashira K, Noumi S, Ito K, Kato D et al.: Quadrilateral space syndrome: a rare complication of thoracic surgery. Ann Thorac Surg 2008; 86: 1350–1351. doi: 10.1016/j.athoracsur.2008.02.039.

17. Ishima T, Usui M, Satoh E, Sakahashi H, Okamura K: Quadrilateral space syndrome caused by a ganglion. J Shoulder Elbow Surg 1998; 7: 80–82. doi: 10.1016/s1058-2746(98)90187-2.

18. Martinoli C, Bianchi S, Pugliese F, Bacigalupo L, Gauglio C, Valle M et al.: Sonography of entrapment neuropathies in the upper limb (wrist excluded). J Clin Ultrasound 2004; 32: 438–450. doi: 10.1002/jcu.20067.

19. Brestas PS, Tsouroulas M, Nikolakopoulou Z, Malagari K, Drossos C: Ultrasound findings of teres minor denervation in suspected quadrilateral space syndrome. J Clin Ultrasound 2006; 34: 343–347. doi: 10.1002/jcu.20239.

20. Desai SS, Arbor TC, Varacallo M: Anatomy, shoulder and upper limb, musculocutaneous nerve. In: StatPearls. StatPearls Publishing 2023.

21. Davidson JJ, Bassett FH 3rd, Nunley JA 2nd: Musculocutaneous nerve entrapment revisited. J Shoulder Elbow Surg 1998; 7: 250–255. doi: 10.1016/s1058-2746(98)90053-2.

22. Pećina M, Bojanić I: Musculocutaneous nerve entrapment in the upper arm. Int Orthop 1993; 17: 232–234. doi: 10.1007/bf00194185.

23. Liveson JA: Nerve lesions associated with shoulder dislocation; an electrodiagnostic study of 11 cases. J Neurol Neurosurg Psychiatry 1984; 47: 742–744. doi: 10.1136/jnnp.47.7.742.

24. Tagliafico AS, Michaud J, Marchetti A, Garello I, Padua L, Martinoli C: US imaging of the musculocutaneous nerve. Skeletal Radiol 2011; 40: 609–616. doi: 10.1007/s00256-010-1046-6.

25. Memon AB, Mahmood S, Waseem F, Sherburn F, Nardone A, Ahmad BK: Lateral antebrachial cutaneous neuropathy: a review of 15 cases. Cureus 2022; 14: e25203. doi: 10.7759/cureus.25203.

26. Chang KV, Mezian K, Naňka O, Wu W-T, Lou Y-M, Wang J-C et al.: Ultrasound imaging for the cutaneous nerves of the extremities and relevant entrapment syndromes: from anatomy to clinical implications. J Clin Med 2018; 7: 457. doi: 10.3390/jcm7110457.

27. Contreras MG, Warner MA, Charbonneau WJ, Cahill DR: Anatomy of the ulnar nerve at the elbow: potential relationship of acute ulnar neuropathy to gender differences. Clin Anat 1998; 11: 372–378. doi: 10.1002/(sici)1098-2353(1998)11:6<372::Aid-ca2>3.0.Co;2-r.

28. Mangi MD, Zadow S, Lim W: Nerve entrapment syndromes of the upper limb: a pictorial review. Insights Imaging 2022; 13: 166. doi: 10.1186/s13244-022-01305-5.

29. Shinohara I, Inui A, Mifune Y, Nishimoto H, Yamaura K, Mukohara S et al.: Diagnosis of cubital tunnel syndrome using deep learning on ultrasonographic images. Diagnostics (Basel) 2022; 12: 632. doi: 10.3390/diagnostics12030632.

30. Staples JR, Calfee R: Cubital tunnel syndrome: current concepts. J Am Acad Orthop Surg 2017; 25: e215–e224. doi: 10.5435/jaaos-d-15-00261.

31. Assmus H, Antoniadis G, Bischoff C, Hoffmann R, Martini A-K, Preissler P et al.: Cubital tunnel syndrome – a review and management guidelines. Cent Eur Neurosurg 2011; 72: 90–98. doi: 10.1055/s-0031-1271800.

32. Mezian K, Jačisko J, Kaiser R, Machač S, Steyerová P, Sobotová K et al.: Ulnar neuropathy at the elbow: from ultrasound scanning to treatment. Front Neurol 2021; 12: 661441. doi: 10.3389/fneur.2021.661441.

33. Zeiss J, Jakab E, Khimji T, Imbriglia J: The ulnar tunnel at the wrist (Guyon's canal): normal MR anatomy and variants. Am J Roentgenol 1992; 158: 1081–1085. doi: 10.2214/ajr.158.5.1566671.

34. Aleksenko D, Varacallo M: Guyon canal syndrome. StatPearls. StatPearls Publishing 2023.

35. Dodds GA, 3rd, Hale D, Jackson WT: Incidence of anatomic variants in Guyon's canal. J Hand Surg Am 1990; 15: 352–355. doi: 10.1016/0363-5023(90)90122-8.

36. Ljungquist KL, Martineau P, Allan C: Radial nerve injuries. J Hand Surg Am 2015; 40: 166–172. doi: 10.1016/j.jhsa.2014.05.010.

37. Levina Y, Dantuluri PK: Radial tunnel syndrome. Curr Rev Musculoskelet Med 2021; 14: 205–213. doi: 10.1007/s12178-021-09703-w

38. Robson AJ, See MS, Ellis H: Applied anatomy of the superficial branch of the radial nerve. Clin Anat 2008; 21: 38–45. doi: 10.1002/ca.20576.

39. Daly M, Langhammer C: Radial nerve injury in humeral shaft fracture. Orthop Clin North Am 2022; 53: 145–154. doi: 10.1016/j.ocl.2022.01.001.

40. Esparza M, Wild JR, Minnock C, Mohty KM, Truchan LM, Taljanovic MS: Ultrasound evaluation of radial nerve palsy associated with humeral shaft fractures to guide operative versus non-operative treatment. Acta Med Acad 2019; 48: 183–192. doi: 10.5644/ama2006-124.257.

41. Bencardino JT, Rosenberg ZS: Entrapment neuropathies of the shoulder and elbow in the athlete. Clin Sports Med 2006; 25: 465–487, vi-vii. doi: 10.1016/j.csm.2006.03.005.

42. Tsai P, Steinberg DR: Median and radial nerve compression about the elbow. Instr Course Lect 2008; 57: 177–185.

43. DeCastro A, Keefe P: Wrist Drop. StatPearls. StatPearls Publishing 2023.

44. Moradi A, Ebrahimzadeh MH, Jupiter JB: Radial tunnel syndrome, diagnostic and treatment dilemma. Arch Bone Jt Surg 2015; 3: 156–162.

45. Kim Y, Ha DH, Lee SM: Ultrasonographic findings of posterior interosseous nerve syndrome. Ultrasonography 2017; 36: 363–369. doi: 10.14366/usg.17007.

46. Anthony JH, Hadeed A, Hoffler CE: Cheiralgia Paresthetica. StatPearls. StatPearls Publishing 2023.

47. Patel A, Pierce P, Chiu DTW: A fascial band implicated in Wartenberg syndrome. Plast Reconstr Surg 2014; 133: 440e–442e. doi: 10.1097/01.prs.0000438497.39857.97.

48. Gurses IA, Coskun O, Gayretli O, Kale A, Ozturk A: The relationship of the superficial radial nerve and its branch to the thumb to the first extensor compartment. J Hand Surg Am 2014; 39: 480–483. doi: 10.1016/j.jhsa.2013.12.004.

49. Murphy KA, Morrisonponce D: Anatomy, Shoulder and Upper Limb, Median Nerve. StatPearls. StatPearls Publishing 2023.

50. Dang AC, Rodner CM: Unusual compression neuropathies of the forearm, part II: median nerve. J Hand Surg Am 2009; 34: 1915–1920. doi: 10.1016/j.jhsa.2009.10.017.

51. Dydyk AM, Negrete G, Sarwan G, Cascella M: Median Nerve Injury. StatPearls. StatPearls Publishing 2023.

52. Rodner CM, Tinsley BA, O'Malley MP: Pronator syndrome and anterior interosseous nerve syndrome. J Am Acad Orthop Surg 2013; 21: 268–275. doi: 10.5435/jaaos-21-05-268.

53. Bilge T, Yalaman O, Bilge S, Cokneşeli B, Barut S: Entrapment neuropathy of the median nerve at the level of the ligament of Struthers. Neurosurgery 1990; 27: 787–789. doi: 10.1097/00006123-199011000-00017.

54. Kowalska B, Sudoł-Szopińska I: Ultrasound assessment on selected peripheral nerve pathologies. Part I: Entrapment neuropathies of the upper limb – excluding carpal tunnel syndrome. J Ultrason 2012; 12: 307–318. doi: 10.15557/JoU.2012.0016.

55. Li N, Russo K, Rando L, Gulotta-Parrish L, Sherman W, Kaye AD: Anterior interosseous nerve syndrome. Orthop Rev (Pavia) 2022; 14: 38678. doi: 10.52965/001c.38678.

56. Na KT, Jang DH, Lee YM, Park IJ, Lee HW, Lee SU: Anterior Interosseous nerve syndrome: is it a compressive neuropathy? Indian J Orthop 2020; 54: 193–198. doi: 10.1007/s43465-020-00099-2.

57. Pham M, Bäumer P, Meinck HM, Schiefer J, Weiler M, Bendszus M et al.: Anterior interosseous nerve syndrome: fascicular motor lesions of median nerve trunk. Neurology 2014; 82: 598–606. doi: 10.1212/wnl.0000000000000128.

58. Dunn AJ, Salonen DC, Anastakis DJ: MR imaging findings of anterior interosseous nerve lesions. Skeletal Radiol 2007; 36: 1155–1162. doi: 10.1007/s00256-007-0382-7.

59. Rodriguez-Niedenführ M, Vazquez T, Parkin I, Logan B, Sañudo JR:. Martin-Gruber anastomosis revisited. Clin Anat 2002; 15: 129–134. doi: 10.1002/ca.1107.

60. Pfirrmann CW, Zanetti M: Variants, pitfalls and asymptomatic findings in wrist and hand imaging. Eur J Radiol 2005; 56: 286–295. doi: 10.1016/j.ejrad.2005.03.010.

61. Presazzi A, Bortolotto C, Zacchino M, Madonia L, Draghi F: Carpal tunnel: normal anatomy, anatomical variants and ultrasound technique. J Ultrasound 2011; 14: 40–46. doi: 10.1016/j.jus.2011.01.006.

62. Genova A, Dix O, Saefan A, Thakur M, Hassan A: Carpal tunnel syndrome: a review of literature. Cureus 2020; 12: e7333. doi: 10.7759/cureus.7333.

63. Wipperman J, Goerl K: Carpal tunnel syndrome: diagnosis and management. Am Fam Physician 2016; 94: 993–999.

64. Petrover D, Richette P: Treatment of carpal tunnel syndrome : from ultrasonography to ultrasound guided carpal tunnel release. Joint Bone Spine 2018; 85: 545–552. doi: 10.1016/j.jbspin.2017.11.003.

65. Serhal A, Serhal M, Samet J: Advanced imaging of upper extremity nerve compression and tunnel syndromes. Adv Clin Radiol 2022; 4: 157–169. doi: 10.1016/j.yacr.2022.05.002.

66. Klauser AS, Halpern EJ, Faschingbauer R, Guerra F, Martinoli C, Gabl MF et al.: Bifid median nerve in carpal tunnel syndrome: assessment with US cross-sectional area measurement. Radiology 2011; 259: 808–815. doi: 10.1148/radiol.11101644.

67. Bayrak IK, Bayrak AO, Kale M, Turker H, Diren B: Bifid median nerve in patients with carpal tunnel syndrome. J Ultrasound Med 2008; 27: 1129–1136. doi: 10.7863/jum.2008.27.8.1129.

68. Salter M, Sinha NR, Szmigielski W: Thrombosed persistent median artery causing carpal tunnel syndrome associated with bifurcated median nerve: aA case report. Pol J Radiol 2011; 76: 46–48.

69. Henry BM, Zwinczewska H, Roy J, Vikse J, Ramakrishnan PK, Walocha JA et al.: The prevalence of anatomical variations of the median nerve in the carpal tunnel: a systematic review and meta-analysis. PLoS One 2015; 10: e0136477. doi: 10.1371/journal.pone.0136477.

70. Mitchell CH, Fayad LM, Ahlawat S: Magnetic resonance imaging of the digital nerves of the hand: anatomy and spectrum of pathology. Curr Probl Diagn Radiol 2018; 47: 42–50. doi: 10.1067/j.cpradiol.2017.02.009.

71. Deshmukh S, Carrino JA, Feinberg JH, Wolfe SW, Eagle S, Sneag DB: pins and needles from fingers to toes: high-resolution mri of peripheral sensory mononeuropathies. Am J Roentgenol 2017; 208: W1–W10. doi: 10.2214/ajr.16.16377.

72. Watson J, Gonzalez M, Romero A, Kerns J: Neuromas of the hand and upper extremity. J Hand Surg Am 2010; 35: 499–510. doi: 10.1016/j.jhsa.2009.12.019.